

Various scenarios for transition to thorium fuel cycle in the Single-fluid Double-zone Thorium Molten Salt Reactor (SD-TMSR)

O. Ashraf^{a,b,*}, Andrei Rykhlevskii^c, G. V. Tikhomirov^a, Kathryn D. Huff^c

^a*Laboratory of Engineering Computer Modeling in Nuclear Technologies, Institute of Nuclear Physics and Engineering, National Research Nuclear University MEPhI, Moscow, Russia, 115409*

^b*Physics Department, Faculty of Education, Ain Shams University, Cairo, Egypt, 11341*

^c*Dept. of Nuclear, Plasma, and Radiological Engineering, University of Illinois at Urbana-Champaign, Urbana, IL 61801, United States*

Abstract

Liquid-fueled Molten Salt Reactor (MSR) systems represent advances in safety, economics, sustainability, and proliferation-resistance. The MSR has been designed to operate in Th/²³³U fuel cycle with ²³³U used as start-up fissile material. Since ²³³U does not exist in nature, it is required to examine other available fissile materials. This work investigated the fuel cycle and neutronics performance of the Single-fluid Double-zone Thorium-based Molten Salt Reactor (SD-TMSR) with different fissile material loadings at start-up: Low-enriched uranium (LEU) (19.79%), Pu mixed with LEU (19.79%), Pu reactor-grade (a mixture of plutonium isotopes chemically extracted from Pressurized Water Reactor (PWR) spent fuel with 33 *GWd/tHM* burnup), Transuranic elements (TRU) from Light Water Reactor (LWR) spent nuclear fuel (SNF) and finally ²³³U. The MSR burnup routine provided by SERPENT-2 has been used to simulate the online reprocessing and refueling in the SD-TMSR. The effective multiplication factor, fuel salt composition evolution and net production of ²³³U have been studied in the present work. The results show that the continuous flow of Pu reactor-grade helps in transition to thorium fuel cycle within a relatively

*Corresponding Author

Email address: osama.ashraf@edu.asu.edu.eg oabdelaziz@mephi.ru (O. Ashraf)

short time (≈ 4.5 years) compared to 26 years for ^{233}U start-up fuel. Finally, using TRU as initial fissile materials shows the possibility of operating the SD-TMSR for a long period of time (≈ 40 years) without any external feed of ^{233}U .

Keywords: MSR, thorium fuel cycle, transmuter, burner, online reprocessing, Monte carlo code

1. Introduction

The Generation IV International Forum (GIF) has defined eight technology goals for the next generation nuclear systems. These goals have been defined in four broad areas: safety and reliability, economics, sustainability, non-proliferation and physical protection [1]. The Molten Salt Reactor (MSR) has many advantages that consistent with GIF's goals, for example, liquid fuel, inherent safety, online reprocessing and refueling, excellent neutron economy and operation near atmospheric pressure in a primary loop [2, 3]. Thus, the GIF selected MSR as one of the promising Generation-IV reactors [1, 4]. In the MSR, the fuel is dissolved in a molten salt (e.g., LiF or NaCl). This liquid fuel salt (e.g., LiF-BeF₂-ThF₄- ^{233}U F₄) constantly circulates through the core and allows transferring fission heat from reactor core to heat exchanger.

The Single-fluid Double-zone Thorium-based Molten Salt Reactor (SD-TMSR-2,250 MW_{th}) was introduced by the Chinese Academy of Sciences (CAS) [5]. The SD-TMSR is a graphite-moderated thermal-spectrum MSR operating in Th/ ^{233}U fuel cycle. In the SD-TMSR the fissile and fertile elements are integrated into the same salt. In addition, the active core is divided into two zones, the radius of the fuel channels in the outer zone is modified to be larger than the radius of the fuel channels in the inner zone to improve the breeding ratio [6, 5].

Historically, the thermal-spectrum MSR was designed for the Th/ ^{233}U fuel cycle [7, 6, 8, 3]. This design assumes that we have fissile ^{233}U inventory to start-up new MSRs. But ^{233}U does not exist in the Earth's crust and can be produced from fertile ^{232}Th only in the nuclear reactor. Therefore, it is

required to examine alternative fissile materials (e.g., ^{235}U) to replace the ^{233}U
 25 in the start-up fuel composition [9, 10]. The thorium fuel cycle transition can
 be achieved after reaching the doubling time¹ of ^{233}U because in this case all
 start-up fissile material is being substituted by newly produced ^{233}U .

Betzler *et al.* discussed the simulation of the start-up of a MSBR unit cell
 with Low-enriched uranium (LEU) (19.79%) and Pu from Light Water Reactor
 30 (LWR) spent fuel (SF) as initial fissile materials [9]. They concluded that the
 plutonium vector extracted from LWR SF is the best alternative source to ^{233}U
 because it has the highest ratio of fissile isotopes [9]. Zou *et al.* introduced two
 approaches for the thorium fuel cycle transition in Thorium-based Molten Salt
 Reactor (TMSR): (1) in-core transition and (2) ex-core transition. In the first
 35 approach, the TMSR is launched with existing fissile material and thorium as a
 fertile material; then the ^{233}U bred from thorium is rerouted into the core to
 maintain criticality. In contrast, the second approach tends to store produced
 ^{233}U out of the core until there is enough amount to start a new TMSR [10].
 Additionally, Zou *et al.* studied the transitioning to thorium fuel cycle in a small
 40 modular Th-based molten salt reactor (smTMSR) using Transuranic elements
 (TRU) as start-up fuel. They concluded that the transition to thorium fuel cycle
 can be achieved in thermal smTMSR with a proper fuel fraction [11].

Heuer *et al.* discussed the transition characteristics of the Molten Salt Fast
 Reactor (MSFR) under different launching scenarios (e.g., enriched uranium
 45 and TRU) they concluded that starting the Thorium fuel cycle is feasible while
 closing the current fuel cycle and adopting stockpile incineration in MSRs for
 optimizing the long-term waste management [12].

Indeed, there are various researches that revolve around starting the MSRs
 with fissile materials alternative to ^{233}U . Many of these researches focus on
 50 the fast-spectrum MSRs [13, 14, 15, 16, 12, 17], while little focus on thermal-
 spectrum MSRs [9, 11, 10]. Nevertheless, starting the Single-fluid Double-zone
 Thorium-based Molten Salt Reactor (SD-TMSR) specifically with other fissile

¹Time required to produce enough amount of ^{233}U to trigger a new SD-TMSR.

materials (except ^{233}U) was not studied before. Therefore, the main object of the present paper is to discuss the simulation of the SD-TMSR operation for a
 55 lifetime-long period of time (60 years) with different initial fissile materials and without any external feed of ^{233}U to achieve the thorium fuel cycle transition. We investigated five different initial fissile materials: LEU, Pu mixed with LEU, Pu reactor-grade, TRU from LWR SF and ^{233}U [18]. Moreover, two different feed scenarios were selected:

- 60 • Continuous feed flow of thorium from Th stockpile and ^{233}U from **Pa-decay tank**², where the removal rate of ^{233}Pa = feed rate of ^{233}U . [9].
- Continuous injection of Heavy Metal (HM) (excluding Th) and simultaneously feed of all or part of produced ^{233}U from **Pa-decay tank**.

All calculations presented in the present paper were performed using SERPENT-
 65 2 version 2.1.30. We used the MSR burnup routine provided by SERPENT-2 to simulate continuous online reprocessing and refueling. SERPENT-2 uses an internal calculation routine for solving the set of Bateman equations describing the changes in the material compositions caused by neutron-induced reactions and radioactive decay [19]. Additionally, SERPENT-2 allows us to
 70 conduct the burnup calculations on computer clusters with multiple cores using distributed-memory MPI parallelization.

This present paper is organized as follows: after an introduction about MSR systems, the model description is discussed in section 2. Methodology and tools is described in section 3. Extraction and feed mechanisms are addressed in section
 75 4. Section 5 focuses on the results and discussion. Finally, section 6 highlights the conclusions.

²An imaginary tank used to store protactinium extracted from the core.

2. Model description

2.1. Geometry

The SD-TMSR design model was introduced by the CAS as a part of the
80 strategic project “Future Advanced Nuclear Energy – Thorium-based Molten
Salt Reactor System (TMSR)” in 2011 [5, 20, 21, 22]. The design of SD-TMSR
is inspired by Molten Salt Breeder Reactor (MSBR) [23] after some modification
in the geometry to control the positive temperature coefficient in MSBR. The
SD-TMSR core geometry was described in details by Li *et al.* [5]. Figure 1
85 illustrates the quarter-core model configuration of the SD-TMSR. The active
zone is a right cylinder with height and diameter equal to 460 cm. Assemblies
of graphite³ hexagonal prisms fill the core. The side length of the graphite
hexagonal prism was optimized in [5] and found to be 7.5 cm. The liquid
fuel circulates continuously through the fuel channels that pierces the graphite
90 hexagonal prisms. The core is divided into two different zones to enhance
Th/²³³U breeding performance. The radius of the fuel channels in the outer and
inner zone are 5 and 3.5 cm, respectively. The axial and radial graphite reflectors
surround the core to minimize neutron leakage and maximize flux in the core.
The reflectors are surrounded by B₄C cylinder that acts as a radiation shielding.
95 The SD-TMSR pressure vessel holds the fuel salt, graphite elements, reflector,
shielding, intermediate heat exchanger (IHx) and made of Ni-based (hastelloy
N) alloy. The main characteristics of the SD-TMSR are listed in Table 1.

2.2. Fuel composition

The general composition of the liquid fuel salt in this work is 70LiF - 17.5BeF₂
100 - 12.5(HM)F₄ mole%, where HM is the heavy metal (mixture of thorium and
other actinides). The aim of this paper is to simulate the operation of SD-TMSR
for 60 years with different start-up fissile compositions and without any external
feed of fissile ²³³U which we assumed is unavailable. For that reason, five different

³We choose graphite density of 2.3 g/cm³, to validate our results against results in the
literature [5, 6].

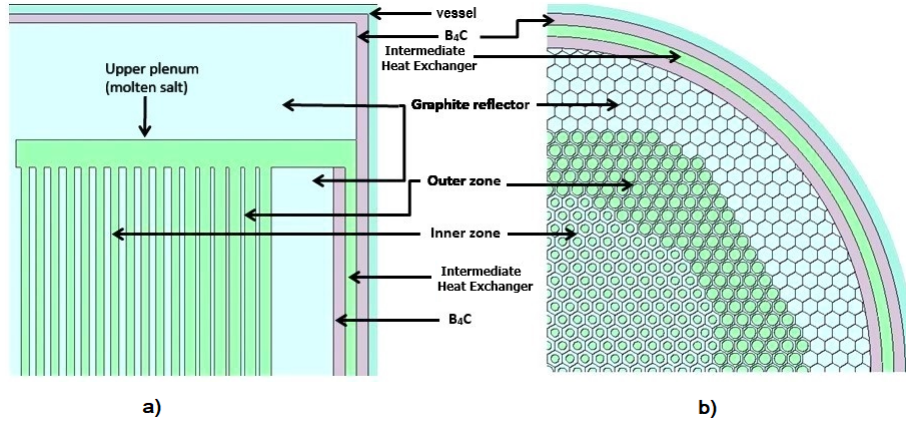


Figure 1: XZ (a) and XY (b) section of the quarter-core model of the SD-TMSR.

Table 1: The main characteristics of the SD-TMSR [5]

| | |
|---|-----------------------|
| Thermal power, MW_{th} | 2,250 |
| Fuel salt components | $LiF-BeF_2-(HM)F_4$ |
| Fuel composition, mole% | 70-17.5-12.5 |
| 7Li enrichment, % | 99.995 |
| Fuel temperature, K | 900 |
| Fuel density at 900 K, g/cm^3 | 3.3 |
| Fuel dilatation coefficient, $g/(cm^3 \cdot K)$ | -6.7×10^{-4} |
| Graphite density, g/cm^3 | 2.3 |
| B_4C density, g/cm^3 | 2.52 |
| ^{10}B enrichment, % | 18.4 |
| Core diameter, cm | 460 |
| Core height, cm | 460 |
| Side length of the graphite hexagonal prism, cm | 7.5 |
| Inner radius, cm | 3.5 |
| Outer radius, cm | 5 |
| Ratio of molten salt and graphite in the inner zone | 0.357 |
| Ratio of molten salt and graphite in the outer zone | 1.162 |
| Fuel volume, m^3 | 52.9 |

Table 2: Reactor-grade plutonium vector (Mass fraction %) [24]

| ^{238}Pu | ^{239}Pu | ^{240}Pu | ^{241}Pu | ^{242}Pu |
|-------------------|-------------------|-------------------|-------------------|-------------------|
| 1.3 | 60.3 | 24.3 | 9.1 | 5 |

Table 3: TRU vector (Mass fraction %) [18]

| ^{237}Np | ^{238}Pu | ^{239}Pu | ^{240}Pu | ^{241}Pu | ^{242}Pu | ^{241}Am | ^{243}Am | ^{244}Cm | ^{245}Cm |
|-------------------|-------------------|-------------------|-------------------|-------------------|-------------------|-------------------|-------------------|-------------------|-------------------|
| 6.3 | 2.7 | 45.9 | 21.5 | 10.7 | 6.7 | 3.4 | 1.9 | 0.8 | 0.1 |

types of initial fissile materials based on LEU, Pu, and TRU from LWR SF were
105 considered:

- (a) low-enriched uranium (LEU) (19.79%);
- (b) Pu mixed with LEU (19.79%);
- (c) Pu reactor-grade [24];
- (d) transuranic (TRU) elements from LWR SF [18];
- 110 (e) ^{233}U for comparison purpose [25].

The reactor-grade plutonium and TRU composition are summarized in Table 2
and 3, respectively.

For reactor-grade plutonium case, the composition was taken for plutonium
recovered from the spent fuel composition of commercial Pressurized Water
115 Reactor (PWR) with the average discharge burnup 33 GWd/t and after 10 years
of cooling before reprocessing [26, 24]. Similarly, the isotopic compositions of
TRU was taken for the SF of UOX PWR (after one use, no multi-recycling)
with the average discharge 60 GWd/t burnup, and after 5 years of cooling [18].
The molar composition of start-up fuel for all five cases is listed in Table 4.
120 Meanwhile, the corresponding initial nuclei inventories with different types of
fuel are summarized in Table 5.

Table 4: Composition of start-up fuel (mole%)

| Fuel component | salt | LEU (19.79%) | Pu+enriched U (19.79wt%) | Pu reactor- grade | TRU | ²³³ U |
|---------------------|------|-----------------|-----------------------------|----------------------|------|------------------|
| LiF | | 70 | 70 | 70 | 70 | 70 |
| BeF ₂ | | 17.5 | 17.5 | 17.5 | 17.5 | 17.5 |
| ThF ₄ | | 8.25 | 7.5 | 10.75 | 8.65 | 12.3 |
| UF ₄ | | 4.25 | 4.75 | | | 0.2 |
| PuF ₃ | | | 0.25 | 1.75 | | |
| (TRU)F ₃ | | | | | 3.85 | |

3. Methodology and tools

Simulation of Liquid-fueled Molten Salt Reactor (MSR) systems requires computational software that must support online fuel salt reprocessing and refueling [27]. In this work, SERPENT-2 version 2.1.31 beta⁴ [19] is used to simulate the full-core of the SD-TMSR with different types of initial fuel. The extension of SERPENT accounts for continuous online reprocessing and refueling [28]. ENDF-VII.0 cross-section library was used for all calculations in this work. The results demonstrate full-core runs of 1.25×10^7 neutron history per depletion step. The full burnup time of the SD-TMSR was 60 years with statistical error in k_{eff} equal to ± 36 pcm. The online extraction of Fission Products (FPs) and other neutron absorbers provides many benefits for MSRs. For example, it would reduce the initial fissile material inventory required to achieve criticality and improve the breeding ratio. Figure 2 shows a flow chart of the calculation steps.

As shown in Figure 2, after launched the input file, an advanced matrix exponential solution based on the Chebyshev Rational Approximation Method (CRAM) [29] used to solve the Bateman equation. Then, the system extracted gaseous FPs and other materials (non-dissolved metals, lanthanides, and soluble

⁴SERPENT-2 is a 3D continuous energy Monte Carlo neutron transport and burnup code.

Table 5: Initial nuclei inventories (in grams) of the SD-TMSR with different types of fuel.

| Molecule | LEU (19.79%) | Pu mixed with en- riched U (19.79%) | Pu reactor- grade | TRU | ²³³ U |
|--|-----------------|--|-------------------------|----------|------------------|
| ²³² Th | 6.24E+07 | 4.67E+07 | 6.75E+07 | 5.44E+07 | 7.69E+07 |
| ²³³ U | | | | | 1.30E+06 |
| ²³⁵ U | 3.17E+06 | 6.01E+06 | | | |
| ²³⁸ U | 1.28E+07 | 2.43E+07 | | | |
| ²³⁷ Np | | | | 1.58E+06 | |
| ²³⁸ Pu | | 1.60E+04 | 1.13E+05 | 6.78E+05 | |
| ²³⁹ Pu | | 9.59E+05 | 6.76E+06 | 1.15E+07 | |
| ²⁴⁰ Pu | | 3.99E+05 | 2.82E+06 | 5.40E+06 | |
| ²⁴¹ Pu | | 1.60E+05 | 1.13E+06 | 2.69E+06 | |
| ²⁴² Pu | | 6.39E+04 | 4.51E+05 | 1.68E+06 | |
| ²⁴¹ Am | | | | 8.53E+05 | |
| ²⁴² Am | | | | | |
| ²⁴³ Am | | | | 4.77E+05 | |
| ²⁴⁴ Cm | | | | 2.01E+05 | |
| ²⁴⁵ Cm | | | | 2.51E+04 | |
| Total mass of HM without ²³² Th | 1.60E+07 | 3.20E+07 | 1.13E+07 | 2.51E+07 | 1.30E+06 |

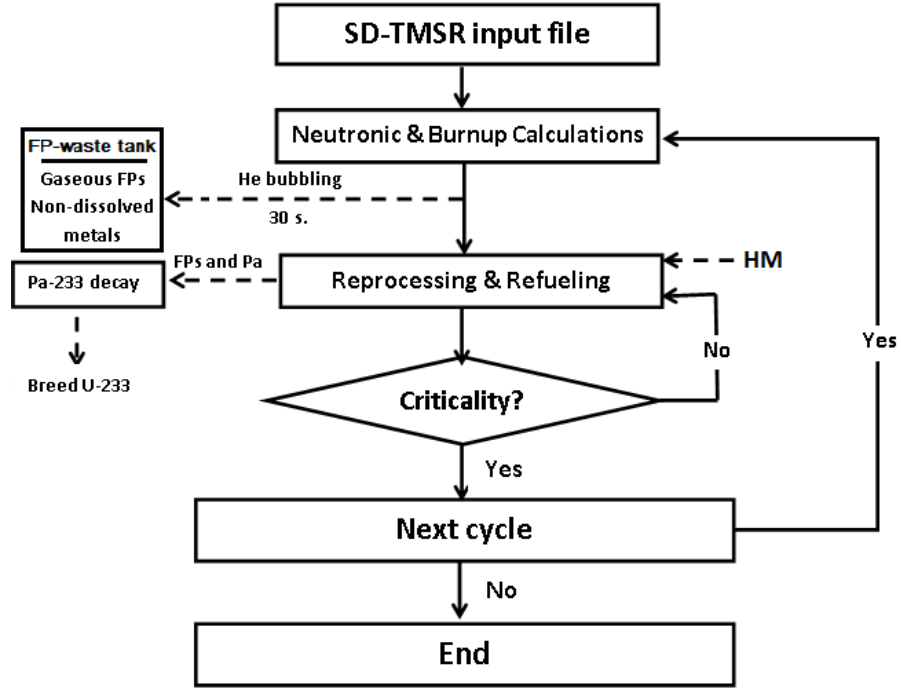


Figure 2: Flow chart of the calculation procedures.

metals except Pu) with suitable removal rate⁵. This can be done by set the flow rate of gaseous FPs and other materials from the fuel to the **FP-waste tank**⁶. Specifically, protactinium was removed from the fuel with a certain flow rate into the external tank, **pa-decay tank**, to decay and produce ^{233}U ⁷. The produced ^{233}U is used as a fresh fissile fuel and the residual ^{233}U is the net production of ^{233}U . The MSR burnup routine provided by SERPENT-2 allows changes the flow rates (*mflow*) of the isotopes during reactor operation [28]. Specifically, we have to determine the mass flow (*mflow*), which is the rate by which elements or nuclides are transferred between materials. After that, the transfer rates should be connected to materials with a reprocessing scheme. Finally, we have to link

⁵The extraction rate depends on the type of poison and its impact on the neutron economy.

⁶An imaginary tank used to store the gaseous FPs and the other materials (non-dissolved metals, lanthanides, and soluble metals except protactinium).

⁷The ^{233}Pa is removed and left to decay into ^{233}U with $\tau_{1/2} \approx 27 d$.

150 the reprocessing schemes to depletion histories. In the present work, we adjusted
the transfer rates of fresh fuel to maintain core criticality and to keep fuel salt
inventory constant during burnup. The feed constant calculation procedures are
summarized as follows:

1. The simulation started without any injection of refueling materials (i.e.
155 with only removing of FPs and Pa).
2. After first depletion calculation step, we checked the total mass density of
FPs and Pa in `FP-waste tank` and `pa-tank`, respectively.
3. A simple calculation yields the amount of Th and ^{233}U that must be added
during this cycle (mass of Th \approx mass of extracted FPs and mass of ^{233}U
160 \approx mass of extracted Pa).
4. Dividing this mass by time and inventory of refueling material gave the
corresponding feed constant.

The cycle calculation ran iteratively until the burnup reached the desired worth.

4. Feed and extraction rates

165 In the present work, two different feed mechanisms are used. The first
mechanism allows continuous feed flow of thorium from Th stockpile, and ^{233}U
from `pa-decay tank`. In contrast, the second mechanism continuously injects
Heavy Metal (HM) (excluding Th) and simultaneously feeds all or part of
produced ^{233}U from `Pa-decay tank`. The fission products act as poisons in
170 the MSRs; they negatively impacting the reactivity. Therefore, FPs must be
extracted during reactor operation. Consider T_r as the time during which the
total fuel salt is reprocessed and dN_e as the amount of particular element e with
inventory N_e that the MSR extracts during time dt ; thus [6]

$$\frac{dN_e}{dt} = N_e \frac{\varepsilon_e}{T_r}, \quad (1)$$

where ε_e is the removal efficiency. Equation 1 gives the removal constant
 175 $\lambda_e [s^{-1}]$ (the rate at which the material is removed), where $\lambda_e = \varepsilon_e/T_r$. The
 removal constant λ_e of gaseous and other fission products is precisely calculated
 and summarized in Table 6. The effective reprocessing time for the gaseous FPs
 and non-dissolved metals was set to 30 seconds (removal constant $\lambda_e = -0.0333$
 s^{-1}), because such elements must be extracted promptly and continuously via
 180 gas removal system. In contrast, extracting the soluble FPs, lanthanides, and
 protactinium can be done by the chemical reprocessing (i.e. fluorination and
 reduction reaction). Therefore, the system reprocesses a specific amount of fuel
 salt daily. In the present work, the effective extraction time for soluble FPs is
 ≈ 10.59 days ($\lambda_e = -1.092 \times 10^{-6} s^{-1}$), which is equivalent to 5 m³/d of chemical
 185 reprocessing rate [6, 5]. The effective feed rates of the heavy metals (HM) are
 changed during reactor operation to conserve the total fuel mass and criticality.
 The effective feed rates for Th/²³³U, Pu reactor-grade and TRU cases are listed
 in Table 10, 11 and 12 in Appendix.

Table 6: The reprocessing table.

| Reprocessing group | Element | Reprocessing time | Removal constant λ_e [s^{-1}] |
|--------------------------------------|--|-----------------------------------|---|
| Gaseous FPs and non-dissolved metals | H, He, N, O, Ne, Ar, Kr, Nb, Mo, Tc, Ru, Rh, Pd, Ag, Sb, Te, Xe, Lu, Hf, Ta, W, Re, Os, Ir, Pt, Au and Rn. | 30s | -3.333E-02 |
| Lanthanides and other soluble FPs | Zn, Ga, Ge, As, Se, Br, Rb, Sr, Y, Zr, Cd, In, Sn, I, Cs, Ba, La, Ce, Pr, Nd, Pm, Sm, Eu, Gd, Tb, Dy, Ho, Er, Tm and Yb. | 10.599 d (5 m ³ /d) | -1.092E-06 |
| Protactinium | Pa | 10.599 d (5 m ³ /d) | -1.092E-06 |

5. Results and discussion

5.1. Thorium feed mechanism

The first mechanism adopts continuous feed flow of external thorium and ^{233}U from **Pa-decay tank**. Hereinafter the first mechanism will be mentioned as the thorium feed mechanism. The molar fraction of the heavy metal in the initial fuel was kept constant and equal to 12.5 mole% for all cases. Besides, the initial fissile material fraction was increased for the five fuel salt compositions until the SD-TMS reactor was sufficiently critical at the Beginning Of Life (BOL). Figure 3 illustrates the change of the effective multiplication with Effective Full-Power Years (EFPY) for the thorium feed mechanism. As shown in Figure 3, the effective multiplication factor (k_{eff}) decreases sharply during the first 25 years of reactor operation for the first four cases. k_{eff} decreases as a result of depletion of the initial fissile materials and generation of the neutron poisons (FPs). Thus, the reactor becomes subcritical within a relatively short time (≈ 4 years in the

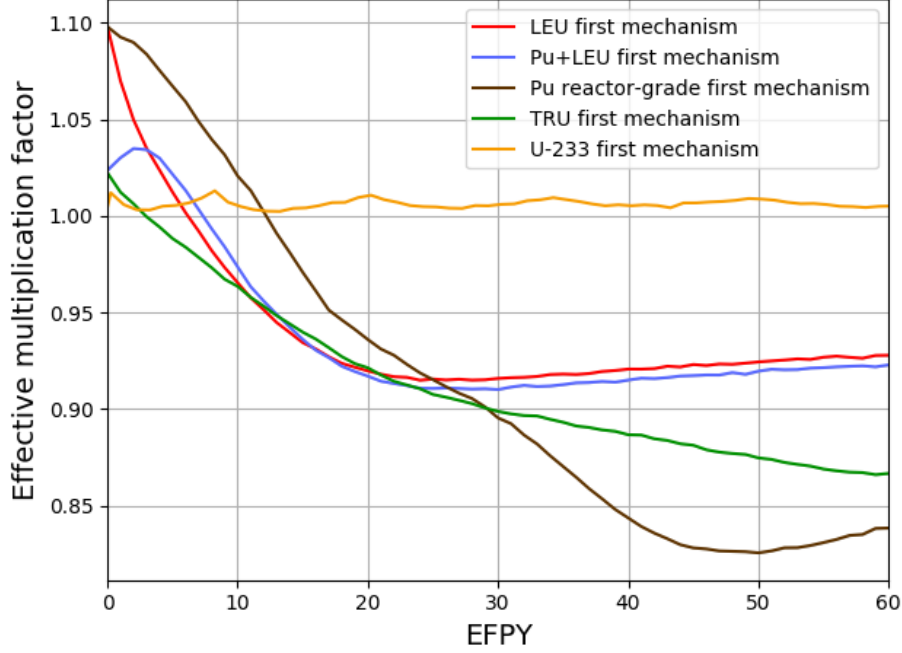


Figure 3: The change of the effective multiplication factor during 60 EFPY of reactor operation for thorium feed mechanism (confidence interval $\pm\sigma$ is shaded).

TRU case and ≈ 12 years in the Pu reactor-grade case). The amount of ^{233}U generated in the SD-TMSR is not enough to conserve the reactor criticality and overcome the neutron absorption in the initial fertile isotopes. Nevertheless, the continuous feed flow of thorium and ^{233}U helps to operate the SD-TMSR for a long period of time (the U-233 case). Additionally, the initial molar fraction in the LEU and Pu reactor-grade cases was increased more (see Figure 3) to counteract the absorption of neutrons in the non-fissile heavy metals added with the initial fuel salt. But k_{eff} still decreases below 1.0, as a result of increasing the non-fissile heavy metals in the initial fuel [9].

5.2. Non-thorium feed mechanism

The second mechanism allows continuous feed flow of ^{233}U from Pa-decay tank and Heavy Metal except for Th. Hereinafter the second mechanism will

215 be mentioned as the non-thorium feed mechanism. Figure 4 shows the change
 of the effective multiplication during 60 EFPY of reactor operation for the
 non-thorium feed mechanism. As shown in Figure 4, the SD-TMS reactor was
 sufficiently critical at the Beginning Of Life (BOL). Both Pu reactor-grade and
 TRU case show promising results relative to the other two cases (i.e. LEU and
 220 Pu+LEU). For the Pu reactor-grade fuel salt, the amount of ^{233}U generated
 in the SD-TMSR in addition to the external feed flow of Pu are sufficient to
 maintain the reactor criticality and overcome the neutron absorption in the
 initial non-fissile isotopes. This may be attributed to the fact that the spectrum
 in the Pu reactor-grade initial core is hardened that is more thorium is being
 225 converted to ^{233}U . For the TRU fuel salt, the amount of ^{233}U and the external
 feed flow of TRU is barely enough to operate the reactor for a long period of time
 (≈ 40 years) without any external feed of ^{233}U . Nevertheless, k_{eff} decreases
 with the burnup because the Minor Actinides⁸ (MA) accumulating in the core as
 a result of continuous TRU feed. As shown in Figure 4, the LEU and Pu+LEU
 230 fuel are less attractive for non-thorium feed mechanism. The continuous LEU
 feed increases the amount of fertile ^{238}U and consequently, reduces the feasibility
 of such fissile materials. The continuous feed of ^{233}U without ^{232}Th will lead
 to supercritical reactor, thus the ^{233}U case is excluded from non-thorium feed
 mechanism.
 235 According to the k_{eff} results, Pu reactor-grade and TRU fissile materials are
 selected and discussed in the following.

5.3. Pu reactor-grade, TRU, and ^{233}U initial fuel

In this section, the simulation of the SD-TMSR with Pu reactor-grade and
 TRU fissile materials is discussed. Besides, the ^{233}U case is listed for comparison.
 240 Figure 5 demonstrates the dynamics of heavy metal refill rate during 60 EFPY
 of SD-TMSR operation. The heavy metal refill rate was adjusted to maintain;

⁸In the present work, the Minor Actinides (MA) include Np, Am and Cm.

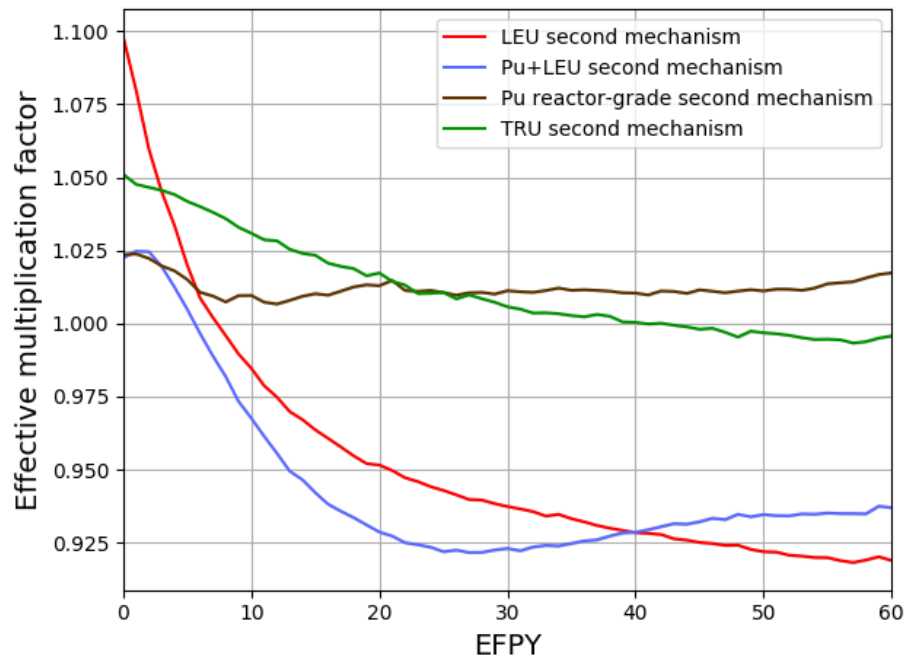


Figure 4: The change of the effective multiplication factor during 60 EFPY of reactor operation for non-thorium feed mechanism (confidence interval $\pm\sigma$ is shaded).

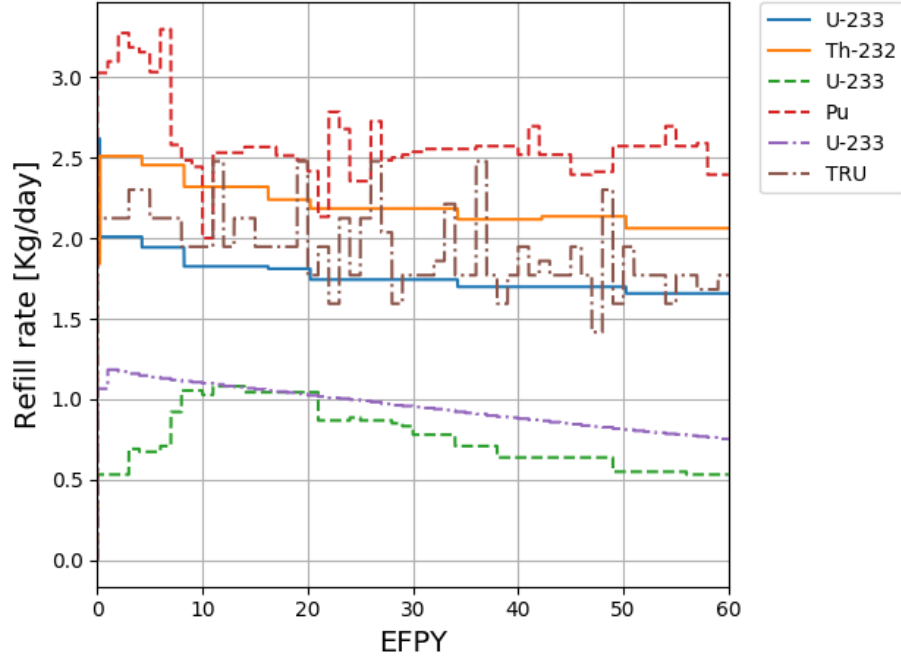


Figure 5: Dynamics of heavy metal refill rate during 60 EFPY of reactor operation. Solid lines for ^{233}U case, dashed lines for Pu reactor-grade case, and dotted lines for TRU case.

the reactor criticality and total fuel mass almost constant⁹ during the reactor operation. In ^{233}U case, the mean values of ^{233}U and ^{232}Th refill rate are 1.77 and 2.21 kg/d , respectively. As well, in the Pu reactor-grade case, the mean values of ^{233}U and Pu refill rate are 0.75 and 2.75 kg/d , respectively. In the TRU case, the mean values of ^{233}U and TRU refill rate are 0.90 and 2.0 kg/d , respectively.

Figure 6 and 7 describe the evolution of important isotopes for ^{233}U , Pu and TRU cases respectively. From Figure 6, the mass of Pa in the fuel salt is almost constant and reaches 17.8 kg at the end of the operation time. In addition, the mass of Minor Actinides (MA) increases with time; however, by applying online reprocessing, its value remains relatively low. As well, the total mass of Pu

⁹The variation of the total fuel mass is less than 0.1%

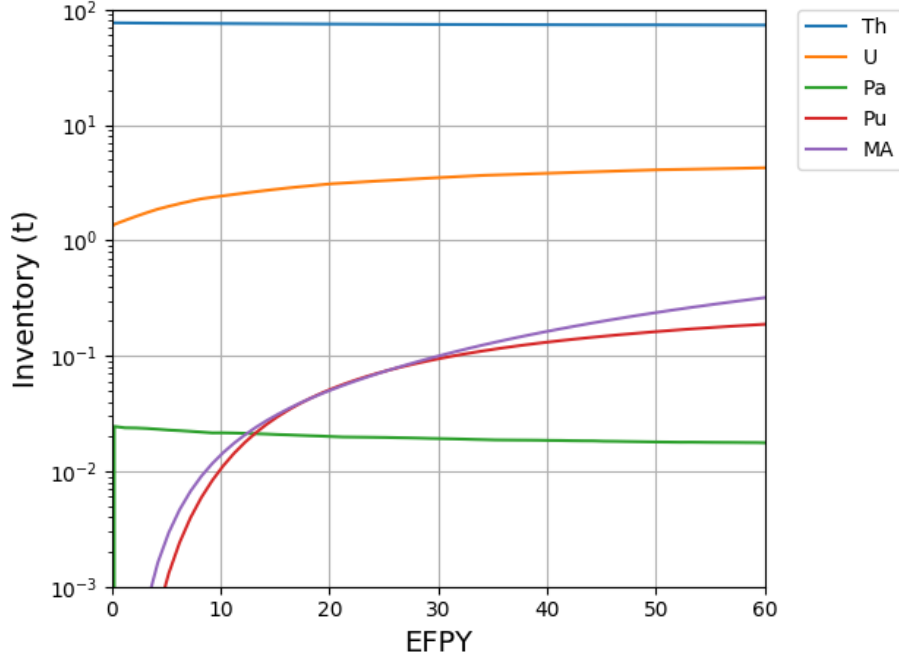


Figure 6: Evolution of the important nuclides inventories for ^{233}U case (MA involves Np, Am, Cm).

increases with burnup. The level of Pu in the fuel correlates with the mass of the MA, and Pu. MA need more time to reach equilibrium. The total mass of U increases with burnup and reaches equilibrium after ≈ 27 years. As shown in Figure 6, refueling the core with Th helps maintain an almost constant inventory throughout the full operation time.

The Pa extraction time was adjusted to be 30 seconds for Pu and TRU cases to avoid poisoning the core. Therefore, Figure 7 shows that the mass of Pa in the fuel for Pu and TRU cases is relatively low when compared to the ^{233}U case. Major isotopes for the three cases reaches the equilibrium state after ≈ 30 years (see Figure 6 and 7).

Figure 8 illustrates the variation of thorium mass in the fuel salt for ^{233}U , Pu reactor-grade and TRU cases, respectively. In ^{233}U case, we apply the thorium feed mechanism, thus thorium mass decreases by only 3.2 % at the end of

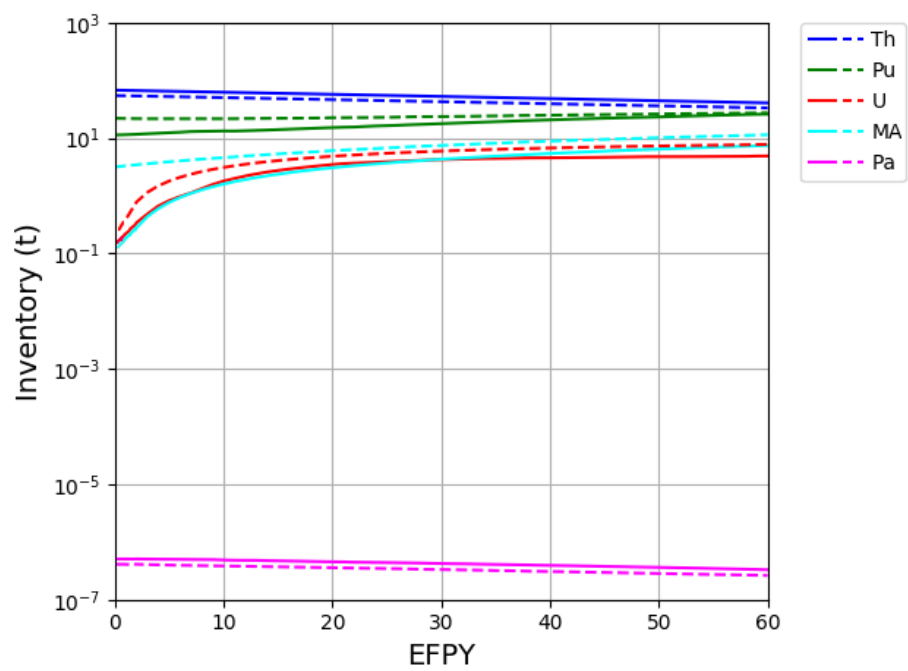


Figure 7: Evolution of the important nuclides inventories for Pu reactor-grade case (solid lines) and for TRU case (dashed lines).

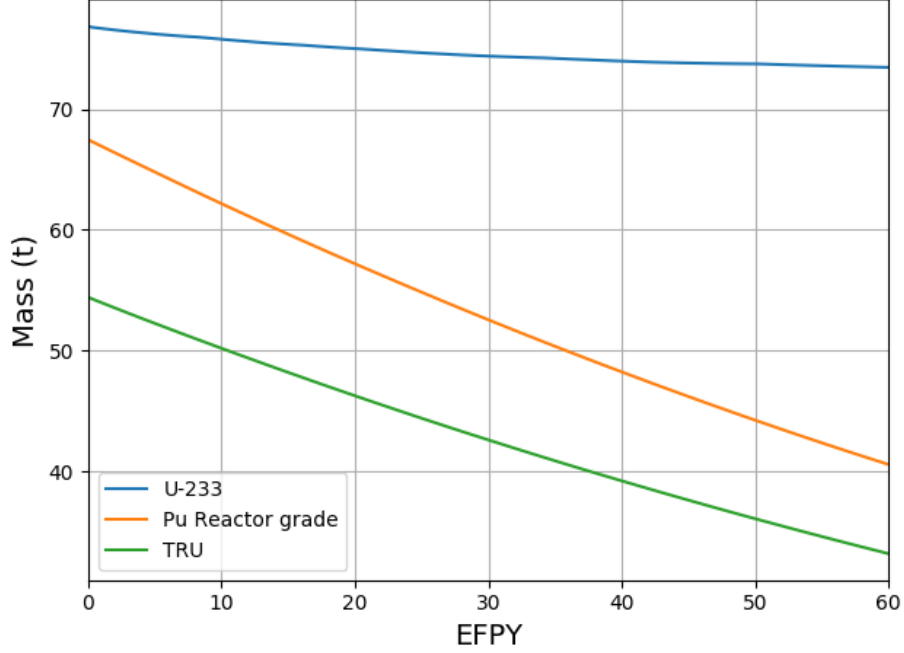


Figure 8: The variation of thorium mass in the fuel salt for ^{233}U , Pu reactor-grade and TRU cases, respectively.

operation time (60 years). In contrast, thorium mass decreases significantly in Pu and TRU cases according to the non-thorium feed mechanism. Thorium mass decreases by 39.2 % and 37.96 % in Pu reactor-grade and TRU cases, respectively. The more decreasing in thorium mass, the more effective utilization
 270 of thorium fuel cycle. Consequently, the Pu reactor-grade initial fuel may help
 to utilize thorium fuel cycle more effective.

Figure 9 demonstrates the mass of ^{233}U in the fuel salt for ^{233}U , Pu reactor-grade and TRU cases, respectively. One can see that the mass of the ^{233}U reaches the equilibrium state after ≈ 30 years. Meanwhile, the amount of ^{233}U
 275 is sufficient to maintain criticality in the three cases.

In the non-thorium feed mechanism, the SD-TMSR is continuously refueled for criticality, which increases the Pu proportion in the molten salt. According to the literature, the limit of Pu solubility in the FLiBe salt is ≈ 4.0 % [30, 31].

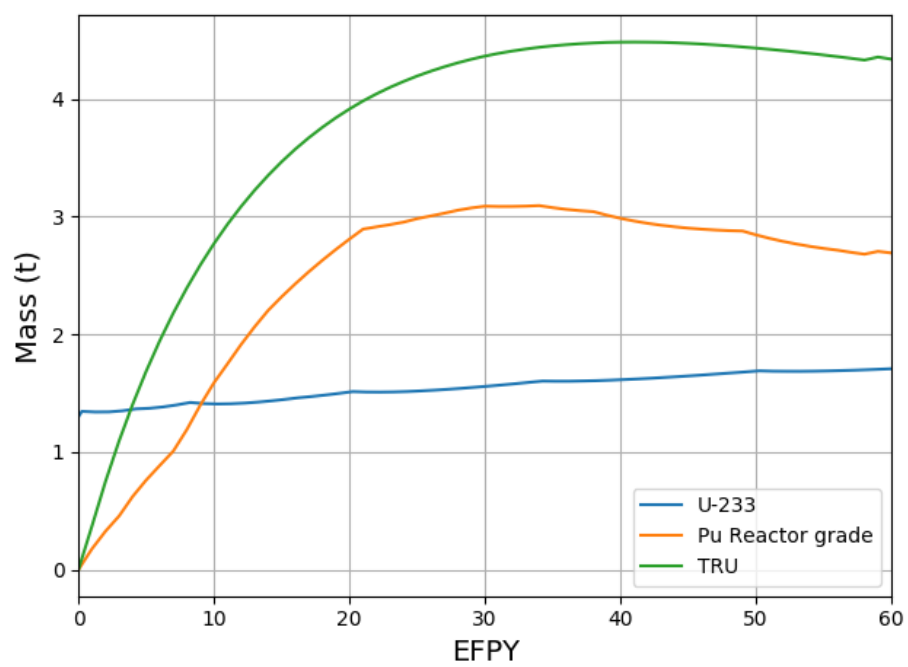


Figure 9: Mass of ^{233}U in the fuel salt for ^{233}U , Pu reactor-grade and TRU case, respectively.

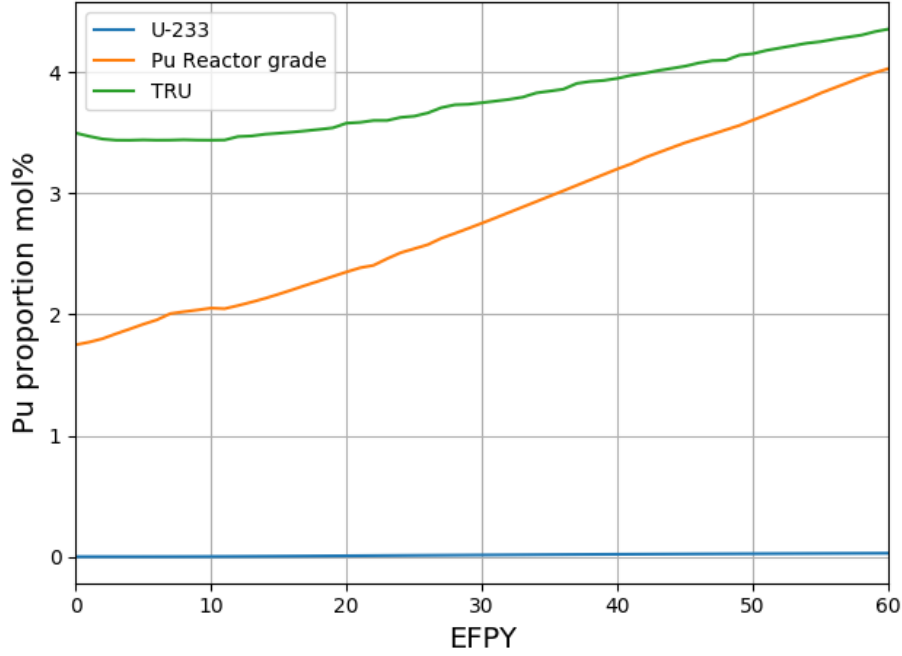


Figure 10: The Pu proportion in the fuel salt (mole%).

Figure 10 represents the Pu proportion in the fuel salt (mole%). In ^{233}U and
 280 Pu reactor-grade cases, the Pu proportion increases slightly but still below
 its solubility limit. On the other hand, the Pu proportion in the molten salt
 loaded by TRU increases with operation time and reaches the Pu solubility limit
 after ≈ 40 years. This issue may be solved by increasing the reactor operation
 temperature and or reducing the HM initial inventory [10].

285 Figure 11 demonstrates the net production of ^{233}U as a function of burnup.
 In TRU case, the net production of ^{233}U is almost zero, nevertheless, the reactor
 becomes subcritical after 40 years of operation. In ^{233}U and Pu reactor-grade
 cases, the net production of ^{233}U increases with burnup and reaches about
 1.77 t and 10 t, respectively at the end of operation lifetime. It worth noting
 290 that thorium feed mechanism is applied in ^{233}U case, while, non-thorium feed
 mechanism is adopted in Pu reactor-grade cases. As shown in Figure 11, after 26
 years the net production of ^{233}U reaches 1.3 t; this is sufficient to start-up another

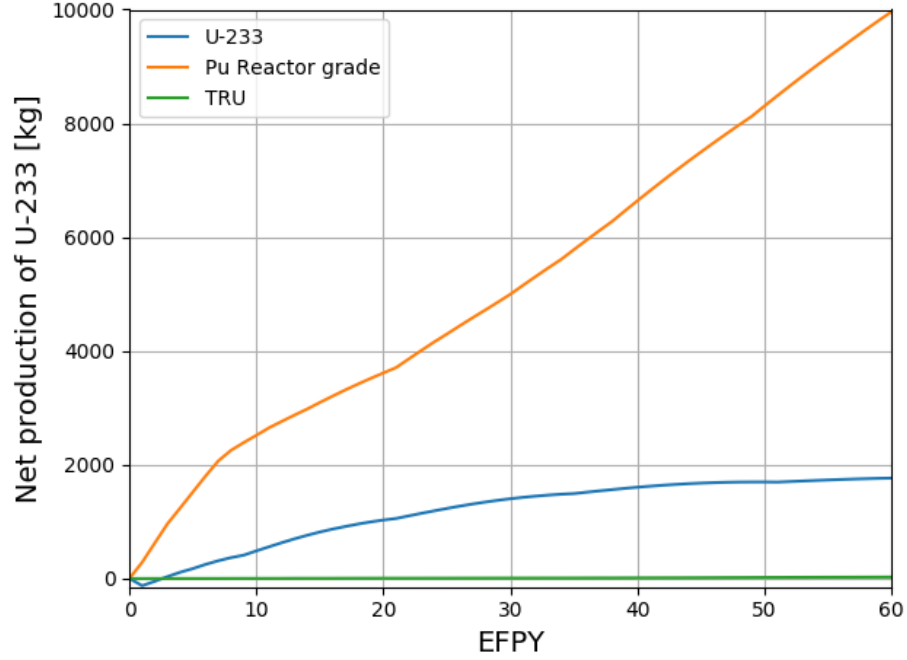


Figure 11: Net production of ^{233}U during burn-up period (60 EFY).

SD-TMSR. Similarly, one can see that the same amount of ^{233}U (i.e. 1.3 t) can be achieved after ≈ 4.5 years if we applied the non-thorium feed mechanism on the SD-TMSR that initially loaded by Pu reactor-grade alternative to ^{233}U . In addition, Figure 11 also shows that the net production of ^{233}U during the first 455 days is negative, thus about 175.28 kg of ^{233}U must be added during this period. In conclusion, the thorium fuel cycle transition can be achieved by selecting the proper feed mechanism and initial fissile material.

5.4. Neutron spectrum

Figure 12 represents the neutron flux per unit lethargy for full-core SD-TMSR model in the energy range from 10^{-8} to 10 MeV for the ^{233}U , Pu reactor-grade, and TRU started case. In ^{233}U case, at the EOL, the neutron spectrum is harder than at BOL due to the accumulation of the Pu and other strong thermal neutron absorbers in the fuel salt. For Pu reactor-grade and TRU cases, during

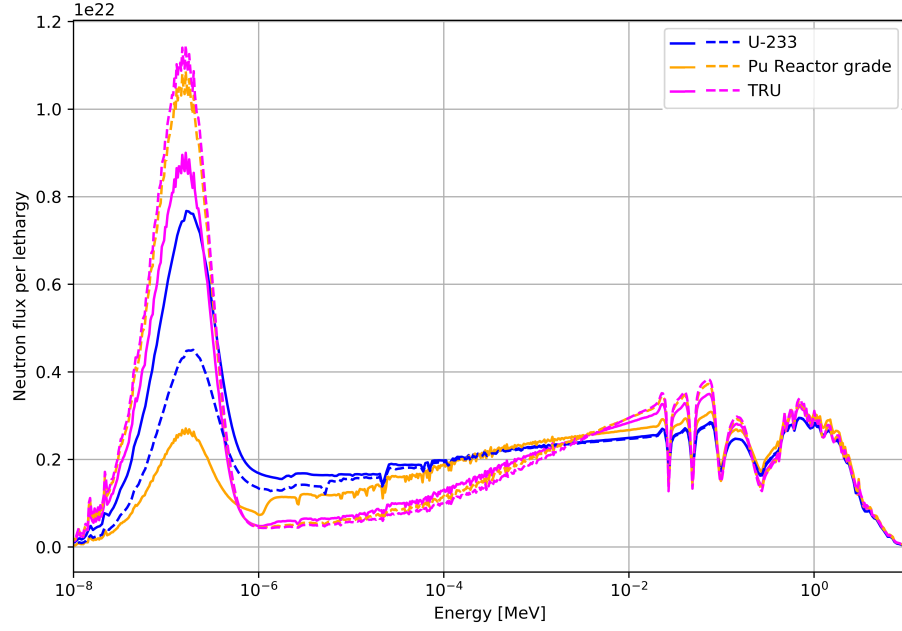


Figure 12: The neutron flux energy spectrum at BOL (solid lines) and EOL (dashed lines) for ^{233}U , Pu reactor-grade, and TRU case.

the reactor operation, the fissile Pu is depleted and the ^{233}U becomes the major fissile isotope (see Figure 9), the neutron spectrum softens and becomes similar to a thermal spectrum of the TMSR.

The comparison between the two feed mechanisms with different types of
 310 initial fuel is listed in Table 7.

Table 7: Comparison between the two feed mechanisms for the five different types of initial fuel.

| Feed mechanism | Initial fuel | LEU | Pu | Pu | TRU | ^{233}U |
|----------------------------|-----------------|-------------|--|---|--|---|
| | | (19.79%) | mixed with en- riched U (19.79 wt-%) | reactor- grade | | |
| Thorium feed mechanism | | Not work | Not work | Not work | Not work | Work |
| Non-thorium feed mechanism | | Not work | Not work | Work well with posi- tive net pro- duc- tion of ^{233}U | Work for 40 <i>years</i> with net pro- duc- tion of ^{233}U = zero | Not exam- ine (su- per- crit- ical reac- tor) |

5.5. Neutron flux

Figures 13, 14 show the radial distribution of fast (energy range between 0.625 eV and 20 MeV) and thermal (energy range between 10^{-5} eV and 0.625 eV) neutron flux for three different initial fissile materials in the fuel salt (^{233}U , reactor-grade plutonium, TRU) at startup and at equilibrium (after ≈ 30 years of operation). Actinides evolution and poisonous fission product accumulation for various initial fissile compositions demonstrated the different effects on the SD-TMSR neutronics performance. For the Th/ ^{233}U , the thermal neutron flux is suppressed at the equilibrium because fissile ^{233}U in the core is being substituted with heavier fissile actinides: ^{235}U , ^{239}Pu , and ^{241}Pu . This is in good agreement with results in the literature [7, 25].

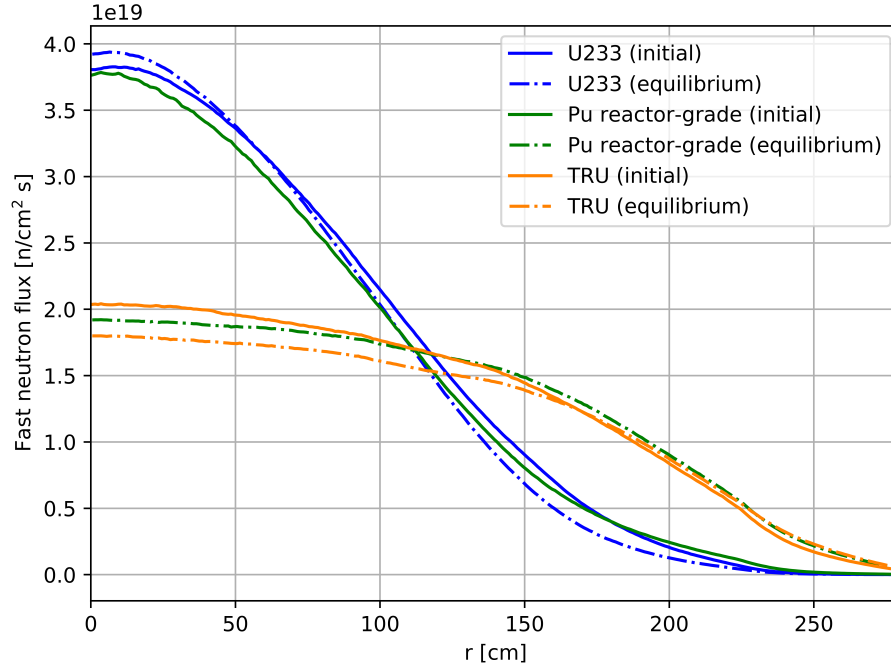


Figure 13: Radial fast neutron flux distribution for 3 different initial fuel salt compositions at startup and equilibrium (the fast flux confidence interval $\pm\sigma < 2.5\%$ for all cases).

Opposite behavior was observed for the Pu reactor-grade and TRU cases. For these cases, the thermal neutron flux is increasing during operation while

fast neutron flux is decreasing. Fissile plutonium nuclides (generate relatively
 325 hard spectrum) from initial fuel salt composition is gradually substituted with
 the ^{233}U (generates relatively soft spectrum), produced from the fertile ^{232}Th .
 During reactor operation, the ^{233}U becomes primary fissile isotope, which leads
 to the neutron spectrum softening of the reactor.

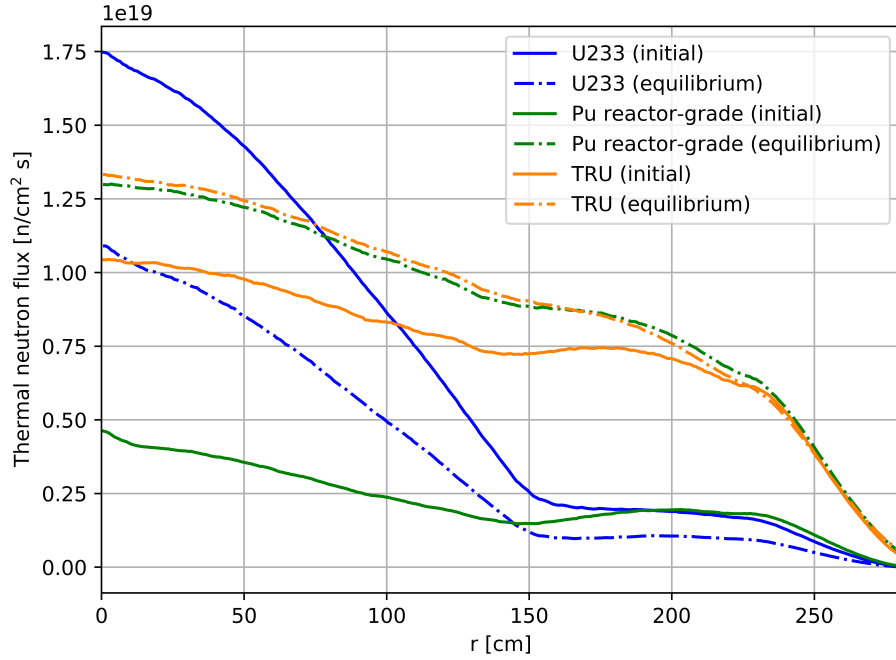


Figure 14: Radial thermal neutron flux distribution for 3 different initial fuel salt compositions at startup and equilibrium (the thermal flux confidence interval $\pm\sigma < 1.6\%$ for all cases).

Notably, more changes in thermal neutron flux shape and magnitude for
 330 ^{233}U case were observed in the inner core zone ($R \lesssim 150$) than in the outer
 core zone. In contrast, for Pu reactor-grade and TRU cases, significant changes
 were observed for thermal neutron flux in the outer core zone and reflector.
 Additionally, Figure 14 shows relatively large changes in thermal flux leakage
 from the core for the Pu and TRU cases. Overall, the SD-TMSR core design was
 335 optimized for ^{233}U fissile isotope [5]; thus, the core geometry (e.g., fuel channels
 lattice pitch) must be re-optimized for another type of fuel to obtain better

neutronics performance.

5.6. Temperature coefficient of reactivity

The temperature coefficient of reactivity quantifies reactivity changes due to temperature increase in the core and was calculated in this work as follows:

$$\alpha = \frac{k_{eff}(T_{i+1}) - k_{eff}(T_i)}{k_{eff}(T_{i+1})k_{eff}(T_i)(T_{i+1} - T_i)} \quad (2)$$

where

k_{eff} = effective multiplication factor

T_i = fuel salt temperature in (900 K, 1000 K).

Table 8 summarizes temperature coefficients calculated for three different initial fissile loads at the startup and at the equilibrium. By propagating the k_{eff} statistical error provided by SERPENT-2, uncertainty for each temperature coefficient was calculated using formula:

$$\delta\alpha = \left| \frac{1}{T_{i+1} - T_i} \right| \sqrt{\frac{\delta k_{eff}^2(T_{i+1})}{k_{eff}^4(T_{i+1})} + \frac{\delta k_{eff}^2(T_i)}{k_{eff}^4(T_i)}} \quad (3)$$

where

δk_{eff} = statistical error for k_{eff} from SERPENT-2 output.

Notably, other sources of uncertainty are neglected, such as cross-section measurement error and approximations inherent in the density dependence on temperature.

When the fuel salt temperature increases, the density of the salt decreases, but at the same time, the total volume of fuel salt in the core remains constant because it is bounded by the vessel. When the graphite temperature increases, the density of graphite decreases, creating additional space for the salt. The cross-section temperatures for the fuel and moderator were changed from 900 to 1000 K to determine the temperature coefficients. This work considered five different cases:

1. Fuel salt temperature (Doppler Effect) rising from 900 to 1000 K (first row in Table 8).
2. Fuel salt density decreasing from 3.3 to 3.233 g/cm³ (density change caused by temperature increase from 900 to 1000 K).
3. Total fuel salt temperature (Doppler+density) rising from 900 to 1000 K.
4. Graphite temperature (Doppler Effect) rising from 900 to 1000 K.
5. Whole reactor temperature rising from 900 K to 1000 K.

In the first case, the fuel temperature change only impacts cross-section temperature. In the second case, changes in the fuel temperature only impact density, and the third case takes into account both effects. The geometry for these three cases is unchanged because the fuel is a liquid. However, when the graphite blocks heat up, both the density and the geometry changing due to the thermal expansion of solid graphite. The graphite linear thermal expansion is not a dominating factor [5], and herein we focus only on Doppler Effect for the moderator temperature coefficient.

The Fuel Temperature Coefficient (FTC) is negative for all considered fuel compositions due to thermal Doppler broadening of the resonance capture cross-

Table 8: Temperature coefficients of reactivity for 3 different initial fuel salt compositions at startup and equilibrium. Confidence interval $\pm\sigma$ for all coefficients is between 0.11 and 0.16 pcm/K).

| Reactivity coefficient (pcm/K) | Startup fissile material | | | | | |
|-----------------------------------|--------------------------|--------|---------|--------|---------|--------|
| | ²³³ U | | Pu | | TRU | |
| | Initial | Equil. | Initial | Equil. | Initial | Equil. |
| Fuel salt temperature | -4.96 | -5.26 | -4.99 | -3.12 | -3.23 | -1.97 |
| Fuel salt density | +1.49 | +2.34 | +1.54 | -1.58 | -0.37 | -1.62 |
| Total salt fuel | -3.77 | -2.83 | -3.22 | -4.23 | -3.25 | -3.69 |
| Graphite temperature | +1.45 | +0.45 | -2.68 | -1.37 | -1.44 | -1.14 |
| Total core | -1.77 | -2.59 | -6.54 | -5.06 | -4.79 | -4.76 |

sections in the thorium. For ^{233}U case, the FTC decreases in magnitude by -25% due to neutron spectrum hardening during the reactor operation. For Pu reactor-grade and TRU cases, the FTC becomes more negative at the equilibrium, by $+31\%$ and $+14\%$, respectively. Spectrum softening for these fueling cases positively affects the FTC magnitude, and this effect seems to be proportional to the spectrum shift.

The Moderator Temperature Coefficient (MTC) for the ^{233}U case is positive and decreases during reactor operation because of spectrum hardening with fuel depletion. For other cases, the MTC is negative and also decreasing in magnitude during the reactor operation. Finally, the total temperature coefficient of reactivity is strongly negative for all considered scenarios but decreases in magnitude during reactor operation due to spectral shift. Notably, the total temperature coefficient is the most negative for the Pu reactor-grade case at startup, which has the hardest neutron spectrum (Figure 12). These coefficients agree with earlier estimates for SD-TMSR [5, 25] and MSBR [7, 32, 23].

Even after 30 years of operation, the total temperature coefficient of reactivity remains relatively large and negative (in the range between -2.59 and -5.06 pcm/K) comparing with the conventional PWR, which has temperature coefficient of about -1.71 pcm/ $^{\circ}\text{F} \approx -3.08$ pcm/K [33]), and allows excellent reactor stability and control. The additional analysis must be performed taking graphite moderator density change and linear thermal expansion into account, but material properties for the SD-TMSR graphite are not available in published literature. Alternatively, relatively well-studied reactor graphite (e.g., AXQ graphite [23]) can be considered as a candidate for the SD-TMSR concept.

5.7. Six Factor analysis

The effective multiplication factor can be expressed as follows:

$$k_{eff} = k_{inf} P_f P_t = \eta f p \epsilon P_f P_t \quad (4)$$

where

η = thermal fission factor

f = thermal utilization factor

p = resonance escape probability

ϵ = fast fission factor

P_f = fast non-leakage probability

P_t = thermal non-leakage probability.

Table 9 summarizes the six factors for 3 different initial fuel salt compositions at startup and equilibrium. By using SERPENT-2 built-in online reprocessing capabilities, all six factors have been calculated at the beginning of the operation and after 30 years of operation. Neutron population and number of
395 active/inactive cycles were selected to obtain k_{eff} statistical uncertainty less than 12 pcm. The fast and thermal non-leakage probabilities remain constant regardless of initial fissile material and neutron spectrum shift during operation. The thermal utilization factor (f) remains almost constant during operation for ^{233}U and TRU cases but considerably declines for Pu case due to significant neutron spectrum softening.

Table 9: Six factors for the SD-TMSR model for 3 different initial fuel salt compositions at startup and equilibrium.

| Factor | Startup fissile material | | | | | |
|------------|--------------------------|-------|---------|-------|---------|-------|
| | ^{233}U | | Pu | | TRU | |
| | Initial | Equil | Initial | Equil | Initial | Equil |
| η | 1.26 | 1.40 | 1.66 | 1.44 | 1.59 | 1.31 |
| f | 0.97 | 0.98 | 0.96 | 0.76 | 0.80 | 0.75 |
| p | 0.54 | 0.43 | 0.26 | 0.16 | 0.17 | 0.15 |
| ϵ | 1.49 | 1.67 | 2.45 | 5.87 | 4.83 | 6.81 |
| P_f | 0.99 | 0.99 | 0.99 | 0.99 | 0.99 | 0.99 |
| P_t | 1.00 | 1.00 | 1.00 | 1.00 | 1.00 | 1.00 |

In contrast, the neutron reproduction factor (η), resonance escape probability (p), and fast fission factor (ϵ) differ notably between initial and equilibrium state for all three initial fissile materials. The fast fission factor (ϵ) is much larger at startup for Pu and TRU cases because these initial fissile materials provided a
405 much harder neutron spectrum than ^{233}U , and ϵ grows throughout the core's lifetime. Conversely, the resonance escape probability decreases during reactor operation. The thermal fission factor increases during reactor operation for the ^{233}U as initial fuel due to the accumulation of fissile plutonium isotopes, which produce more neutrons per fission (ν). The other two scenarios demonstrated
410 opposite behavior: plutonium isotopes with large neutrons per fission production (ν) are gradually substituted with the ^{233}U , which has lower ν [34]. This six factors' evolution agrees with previously determined evolution parameters for a similar single-fluid double-zone MSBR [25, 7, 35].

6. Conclusion

415 In the present paper, five different types of initial fissile materials have been studied for transitioning to thorium fuel cycle in the SD-TMSR. The molar composition of start-up fuel for all five cases is listed in Table 4, as well, the inventories in Table 5. We adopted two different feed mechanisms; thorium feed mechanism and non-thorium feed mechanism. The whole-core of the SD-TMSR
420 was simulated with Pu reactor-grade, TRU, and ^{233}U as initial fissile materials. Additionally, the variation of the effective multiplication factor k_{eff} , inventory, and other neutronic parameters have been investigated. Results demonstrated that continuous flow of Pu reactor-grade helps in transition to thorium fuel cycle within a relatively short time (≈ 4.5 years) compared to 26 years for
425 Th/ ^{233}U start-up fuel. Meanwhile, using TRU as initial fissile materials shows the possibility of operating the SD-TMSR for a long period of time (≈ 40 years) without any external feed of ^{233}U . In addition, the Pu proportion in fuel salt has been calculated and found to be below the solubility limit. Finally, the neutron spectrum shift during the reactor operation for the three selected cases has been

430 calculated.

7. Future work

8. Conflict of interest

The authors declare no conflict of interest.

9. Acknowledgments

435 Osama Ashraf would like to thank the Egyptian Ministry of Higher Education (MoHE), as well as MEPHI's Competitiveness Program for providing financial support for this research. The facility and tools needed to conduct this work were supported by MEPHI.

The authors contributed to this work as described below.

440 Osama Ashraf conceived and designed the simulations, wrote the paper, prepared figures and/or tables, performed the computation work, and reviewed drafts of the paper.

Andrei Rykhlevskii conceived and designed the simulations, wrote the paper, prepared figures and/or tables, performed the computation work, and
445 reviewed drafts of the paper. Andrei Rykhlevskii is supported by DOE ARPA-E MEITNER program award DE-AR0000983.

G. V. Tikhomirov directed and supervised the work, conceived and designed the simulations and reviewed drafts of the paper. Prof. Tikhomirov is supported by Rosatom, he is Deputy Director of the Institute of Nuclear Physics and
450 Engineering MEPHI. Board member of Nuclear society of Russia.

Kathryn D. Huff supervised the work, conceived and contributed to conception of the simulations, and reviewed drafts of the paper. Prof. Huff is supported by the Nuclear Regulatory Commission Faculty Development Program, the National Center for Supercomputing Applications, the NNSA Office of Defense Nuclear
455 Nonproliferation R&D through the Consortium for Verification Technologies and the Consortium for Nonproliferation Enabling Capabilities, the International

Institute for Carbon Neutral Energy Research (WPI-I2CNER), sponsored by the Japanese Ministry of Education, Culture, Sports, Science and Technology, and DOE ARPA-E MEITNER program award DE-AR0000983.

460 This research is part of the Blue Waters sustained-petascale computing project, which is supported by the National Science Foundation (awards OCI-0725070 and ACI-1238993) and the state of Illinois. Blue Waters is a joint effort of the University of Illinois at Urbana-Champaign and its National Center for Supercomputing Applications

465 **10. Appendix**

Table 10: The refueling table for Th/²³³U case

| Nuclide | Feed rate | Feed constant* $\lambda_e [s^{-1}]$ |
|-------------------|---|--|
| ²³² Th | 1.842 [Kg/day], first 90 [d] | 1.500E-09 |
| | 2.511 [Kg/day], from 90 to 1550 [d] | 2.045E-09 |
| | 2.456 [Kg/day], from 1550 to 3010 [d] | 2.000E-09 |
| | 2.321 [Kg/day], from 3010 to 5930 [d] | 1.890E-09 |
| | 2.241 [Kg/day], from 5930 to 7390 [d] | 1.825E-09 |
| | 2.186 [Kg/day], from 7390 to 12500 [d] | 1.780E-09 |
| | 2.118 [Kg/day], from 12500 to 15420 [d] | 1.725E-09 |
| | 2.136 [Kg/day], from 15420 to 18340 [d] | 1.740E-09 |
| | 2.063 [Kg/day], from 18340 to 21900 [d] | 1.680E-09 |
| ²³³ U | 2.619 [Kg/day], first 90 [d] | 6.400E-09 |
| | 2.009 [Kg/day], form 90 to 1550 [d] | 4.910E-09 |
| | 1.944 [Kg/day], from 1550 to 3010 [d] | 4.750E-09 |
| | 1.826 [Kg/day], from 3010 to 5930 [d] | 4.460E-09 |
| | 1.811 [Kg/day], from 5930 to 7390[d] | 4.425E-09 |
| | 1.744 [Kg/day], from 7390 to 12500 [d] | 4.260E-09 |
| | 1.699 [Kg/day], from 12500 to 18340 [d] | 4.150E-09 |
| | 1.657 [Kg/day], from 18340 to 21900 [d] | 4.050E-09 |

* Feed constant is the mass fraction of fertile or fissile nuclides (²³²Th or ²³³U) transferred from the external storage to the core per second.

Table 11: The refueling table for Pu reactor-grade case.

| Nuclide | Feed rate | Feed constant* $\lambda_e [s^{-1}]$ |
|---------|---|---|
| Pu | 3.028 [Kg/day], first 365 [d] | 1.71E-08 |
| | 3.099 [Kg/day], from 365 to 730 [d] | 1.75E-08 |
| | 3.276 [Kg/day], from 730 to 1095 [d] | 1.85E-08 |
| | 3.188 [Kg/day], from 1095 to 1460 [d] | 1.80E-08 |
| | 3.158 [Kg/day], from 1460 to 1825 [d] | 1.78E-08 |
| | 3.034 [Kg/day], from 1825 to 2190 [d] | 1.71E-08 |
| | 3.299 [Kg/day], from 2190 to 2555 [d] | 1.86E-08 |
| | 2.581 [Kg/day], from 2555 to 2920 [d] | 1.46E-08 |
| | 2.484 [Kg/day], from 2920 to 3285 [d] | 1.40E-08 |
| | 2.444 [Kg/day], from 3285 to 3650 [d] | 1.38E-08 |
| | 2 [Kg/day], from 3650 to 4015 [d] | 1.13E-08 |
| | 2.532 [Kg/day], from 4015 to 5110 [d] | 1.43E-08 |
| | 2.568 [Kg/day], from 5110 to 6205 [d] | 1.45E-08 |
| | 2.515 [Kg/day], from 6205 to 6935 [d] | 1.42E-08 |
| | 2.483 [Kg/day], from 6935 to 7300 [d] | 1.40E-08 |
| | 2.417 [Kg/day], from 7300 to 7665 [d] | 1.37E-08 |
| | 2.134 [Kg/day], from 7665 to 8030 [d] | 1.21E-08 |
| | 2.786 [Kg/day], from 8030 to 8395 [d] | 1.57E-08 |
| | 2.679 [Kg/day], from 8395 to 8760 [d] | 1.51E-08 |
| | 2.355 [Kg/day], from 8760 to 9490 [d] | 1.33E-08 |
| | 2.727 [Kg/day], from 9490 to 9855 [d] | 1.54E-08 |
| | 2.484 [Kg/day], from 9855 to 10220 [d] | 1.40E-08 |
| | 2.502 [Kg/day], from 10220 to 10585 [d] | 1.41E-08 |
| | 2.520 [Kg/day], from 10585 to 10950 [d] | 1.42E-08 |
| | 2.538 [Kg/day], from 10950 to 11315 [d] | 1.43E-08 |
| | 2.555 [Kg/day], from 11315 to 13140 [d] | 1.44E-08 |
| | 2.573 [Kg/day], from 13140 to 14600 [d] | 1.45E-08 |
| | 2.520 [Kg/day], from 14600 to 16425 [d] | 1.42E-08 |
| | 2.396 [Kg/day], from 16425 to 17155 [d] | 1.35E-08 |
| | 2.414 [Kg/day], from 17155 to 17885 [d] | 1.36E-08 |
| | 2.573 [Kg/day], from 17885 to 19710 [d] | 1.45E-08 |
| | 2.697 [Kg/day], from 19710 to 20075 [d] | 1.52E-08 |
| | 2.573 [Kg/day], from 20075 to 21170 [d] | 1.45E-08 |

Table 12: The refueling table for TRU case.

| Nuclide | Feed rate | Feed constant* $\lambda_e [s^{-1}]$ |
|---------|---|---|
| TRU | 2.125 [Kg/day], first 365 to 1095 [d] | 1.20E-08 |
| | 2.302 [Kg/day], from 1095 to 1825 [d] | 1.30E-08 |
| | 2.125 [Kg/day], from 1825 to 2920 [d] | 1.20E-08 |
| | 1.9488 [Kg/day], from 2920 to 4015 [d] | 1.10E-08 |
| | 2.479 [Kg/day], from 4015 to 4380 [d] | 1.40E-08 |
| | 1.948 [Kg/day], from 4380 to 4745 [d] | 1.10E-08 |
| | 2.125 [Kg/day], from 4745 to 5110 [d] | 1.20E-08 |
| | 1.948 [Kg/day], from 5110 to 6935 [d] | 1.10E-08 |
| | 2.479 [Kg/day], from 6935 to 7300 [d] | 1.40E-08 |
| | 1.771 [Kg/day], from 7300 to 7665 [d] | 1.00E-08 |
| | 1.948 [Kg/day], from 7665 to 8030 [d] | 1.10E-08 |
| | 1.594 [Kg/day], from 8030 to 8395 [d] | 0.90E-08 |
| | 2.125 [Kg/day], from 8395 to 8760 [d] | 1.20E-08 |
| | 1.771 [Kg/day], from 8760 to 9125 [d] | 1.00E-08 |
| | 2.125 [Kg/day], from 9125 to 9490 [d] | 1.20E-08 |
| | 2.479 [Kg/day], from 9490 to 9855 [d] | 1.4E-08 |
| | 2.036 [Kg/day], from 9855 to 10220 [d] | 1.15E-08 |
| | 1.594 [Kg/day], from 10220 to 10585 [d] | 0.90E-08 |
| | 1.771 [Kg/day], from 10585 to 11680 [d] | 1.00E-08 |
| | 1.859 [Kg/day], from 11680 to 12045 [d] | 1.05E-08 |
| | 2.214 [Kg/day], from 12045 to 12410 [d] | 1.25E-08 |
| | 1.771 [Kg/day], from 12410 to 13140 [d] | 1.00E-08 |
| | 2.479 [Kg/day], from 13140 to 13505 [d] | 1.40E-08 |
| | 1.771 [Kg/day], from 13505 to 13870 [d] | 1.00E-08 |
| | 1.594 [Kg/day], from 13870 to 14235 [d] | 0.90E-08 |
| | 1.771 [Kg/day], from 14235 to 14600 [d] | 1.00E-08 |
| | 1.948 [Kg/day], from 14600 to 14965 [d] | 1.10E-08 |
| | 1.771 [Kg/day], from 14965 to 17155 [d] | 1.00E-08 |
| | 1.416 [Kg/day], from 17155 to 17520 [d] | 0.80E-08 |
| | 2.302 [Kg/day], from 17520 to 17885 [d] | 1.30E-08 |
| | 1.594 [Kg/day], from 17885 to 18250 [d] | 0.90E-08 |
| | 1.771 [Kg/day], from 18250 to 20440 [d] | 1.00E-08 |
| | 1.594 [Kg/day], from 20440 to 21170 [d] | 0.90E-08 |

References

- [1] DOE, US, A technology roadmap for generation iv nuclear energy systems (2002) 48–52.
- [2] D. D. Siemer, Why the molten salt fast reactor (msfr) is the best gen iv reactor, *Energy Science & Engineering* 3 (2) (2015) 83–97.
- [3] M. Rosenthal, P. Kasten, R. Briggs, Molten-salt reactorshistory, status, and potential, *Nuclear Applications and Technology* 8 (2) (1970) 107–117.
- [4] I. Pioro, Handbook of generation IV nuclear reactors, Woodhead Publishing, 2016.
- [5] G. C. Li, P. Cong, C. G. Yu, Y. Zou, J. Y. Sun, J. G. Chen, H. J. Xu, Optimization of Th-U fuel breeding based on a single-fluid double-zone thorium molten salt reactor, *Progress in Nuclear Energy* 108 (2018) 144–151. doi:10.1016/j.pnucene.2018.04.017.
URL <http://www.sciencedirect.com/science/article/pii/S0149197018300970>
- [6] A. Nuttin, D. Heuer, A. Billebaud, R. Brissot, C. Le Brun, E. Liatard, J.-M. Loiseaux, L. Mathieu, O. Meplan, E. Merle-Lucotte, et al., Potential of thorium molten salt reactorsdetailed calculations and concept evolution with a view to large scale energy production, *Progress in nuclear energy* 46 (1) (2005) 77–99.
- [7] A. Rykhlevskii, J. W. Bae, K. D. Huff, Modeling and simulation of online reprocessing in the thorium-fueled molten salt breeder reactor, *Annals of Nuclear Energy* 128 (2019) 366–379. doi:10.1016/j.anucene.2019.01.030.
- [8] E. Merle-Lucotte, D. Heuer, C. Le Brun, J. Loiseaux, Scenarios for a worldwide deployment of nuclear energy production.

- [9] B. R. Betzler, J. J. Powers, A. Worrall, Modeling and simulation of the start-up of a thorium-based molten salt reactor, in: Proc. Int. Conf. PHYSOR, 2016.
- 495 [10] C. Zou, C. Cai, C. Yu, J. Wu, J. Chen, Transition to thorium fuel cycle for tmsr, Nuclear Engineering and Design 330 (2018) 420–428.
- [11] C. Zou, G. Zhu, C. Yu, Y. Zou, J. Chen, Preliminary study on trus utilization in a small modular th-based molten salt reactor (smtmsr), Nuclear Engineering and Design 339 (2018) 75–82.
- 500 [12] D. Heuer, E. Merle-Lucotte, M. Allibert, M. Brovchenko, V. Ghetta, P. Rubiolo, Towards the thorium fuel cycle with molten salt fast reactors, Annals of Nuclear Energy 64 (2014) 421–429.
- [13] O. Ashraf, A. Smirnov, G. Tikhomirov, Modeling and criticality calculation of the molten salt fast reactor using serpent code, in: Journal of Physics: Conference Series, Vol. 1189, IOP Publishing, 2019, p. 012007.
- 505 [14] O. Ashraf, A. Smirnov, G. Tikhomirov, Nuclear fuel optimization for molten salt fast reactor, in: Journal of Physics: Conference Series, Vol. 1133, IOP Publishing, 2018, p. 012026. doi:doi:10.1088/1742-6596/1133/1/012026.
- 510 [15] A. Rykhlevskii, B. R. Betzler, A. Worrall, K. D. Huff, Fuel Cycle Performance of Fast Spectrum Molten Salt Reactor Designs, in: Proceedings of Mathematics and Computation 2019, American Nuclear Society, Portland, OR, 2019.
- [16] B. R. Betzler, A. Rykhlevskii, A. Worrall, K. Huff, Impacts of Fast-Spectrum Molten Salt Reactor Characteristics on Fuel Cycle Performance, Tech. rep., 515 Oak Ridge National Lab.(ORNL), Oak Ridge, TN (United States) (2019).
- [17] C. Fiorina, M. Aufiero, A. Cammi, F. Franceschini, J. Krepel, L. Luzzi, K. Mikityuk, M. E. Ricotti, Investigation of the msfr core physics and fuel cycle characteristics, Progress in Nuclear Energy 68 (2013) 153–168.

- 520 [18] C. de Saint Jean, M. Delpech, J. Tommasi, G. Youinou, P. Bourdot,
Scénarios cne: réacteurs classiques, caractérisation à l'équilibre, rapport
CEA DER/SPRC/LEDC/99-448.
- [19] J. Leppänen, M. Pusa, T. Viitanen, V. Valtavirta, T. Kaltiaisenaho, The
serpent monte carlo code: Status, development and applications in 2013,
525 in: SNA+ MC 2013-Joint International Conference on Supercomputing in
Nuclear Applications+ Monte Carlo, EDP Sciences, 2014, p. 06021.
- [20] M. Jiang, H. Xu, Z. Dai, Advanced fission energy program-tmsr nuclear
energy system, Bull. Chin. Acad. Sci 27 (3) (2012) 366–374.
- [21] X. Li, X. Cai, D. Jiang, Y. Ma, J. Huang, C. Zou, C. Yu, J. Han, J. Chen,
530 Analysis of thorium and uranium based nuclear fuel options in fluoride
salt-cooled high-temperature reactor, Progress in Nuclear Energy 78 (2015)
285–290.
- [22] G. Li, Y. Zou, C. Yu, et al., Model optimization and analysis of th-u
breeding based on msfr, Nucl. Tech 40 (2017) 020603–020603.
- 535 [23] R. C. Robertson, Conceptual Design Study of a Single-Fluid Molten-Salt
Breeder Reactor., Tech. Rep. ORNL-4541, comp.; Oak Ridge National
Laboratory, Tenn. (Jan. 1971).
URL <http://www.osti.gov/scitech/biblio/4030941>
- [24] J. C. Marka, Explosive properties of reactor-grade plutonium, Science &
540 Global Security 4 (1) (1993) 111–128.
- [25] O. Ashraf, A. Rykhlevskii, G. Tikhomirov, K. D. Huff, Whole core analysis
of the single-fluid double-zone thorium molten salt reactor (sd-tmsr), Annals
of Nuclear Energy.
- [26] N. OECD, Probabilistic safety assessment in nuclear power plant manage-
545 ment: a report by a group of experts of the nea committee on the safety of
nuclear installations, june 1989, 112 (1989).

- [27] J. Serp, M. Allibert, O. Beneš, S. Delpech, O. Feynberg, V. Ghetta, D. Heuer, D. Holcomb, V. Ignatiev, J. L. Kloosterman, et al., The molten salt reactor (msr) in generation iv: overview and perspectives, *Progress in Nuclear Energy* 77 (2014) 308–319.
- [28] M. Aufiero, A. Cammi, C. Fiorina, J. Leppänen, L. Luzzi, M. E. Ricotti, An extended version of the serpent-2 code to investigate fuel burn-up and core material evolution of the molten salt fast reactor, *Journal of Nuclear Materials* 441 (1-3) (2013) 473–486.
- [29] A. Isotalo, M. Pusa, Improving the accuracy of the chebyshev rational approximation method using substeps, *Nuclear Science and Engineering* 183 (1) (2016) 65–77.
- [30] V. Ignatiev, O. Feynberg, A. Merzlyakov, A. Surenkov, A. Zagnitko, V. Afonichkin, A. Bovet, V. Khokhlov, V. Subbotin, R. Fazilov, et al., Progress in development of mosart concept with th support, in: *Proceedings of ICAPP*, Vol. 12394, 2012.
- [31] D. Sood, P. Iyer, R. Prasad, V. Vaidya, K. Roy, V. Venugopal, Z. Singh, M. Ramaniah, Plutonium trifluoride as a fuel for molten salt reactors-solubility studies, *Nuclear technology* 27 (3) (1975) 411–415.
- [32] A. Rykhlevskii, A. Lindsay, K. D. Huff, Full-core analysis of thorium-fueled Molten Salt Breeder Reactor using the SERPENT 2 Monte Carlo code, in: *Transactions of the American Nuclear Society*, American Nuclear Society, Washington, DC, United States, 2017.
- [33] B. Forget, K. Smith, S. Kumar, M. Rathbun, J. Liang, Integral Full Core Multi-Physics PWR Benchmark with Measured Data, Tech. rep., Massachusetts Institute of Technology (2018).
- [34] N. G. Sjöstrand, J. S. Story, Cross sections and neutron yields for U-233, U-235 and Pu-239 at 2200 m/sec, Tech. rep., AB Atomenergi (1960).

- [35] J. Park, Y. Jeong, H. C. Lee, D. Lee, Whole core analysis of molten salt breeder reactor with online fuel reprocessing, International Journal of Energy Research 39 (12) (2015) 1673–1680. doi:10.1002/er.3371.
URL <http://doi.wiley.com/10.1002/er.3371>